# Magnetic Topology in November 5, 1998 Two-Ribbon Flare as Inferred from Ground-Based Observations and Linear Force-Free Field Modeling

V. B. Yurchyshyn[1,2], H. Wang [1], J. Qiu [1], P. R. Goode [1]
[1]Big Bear Solar Observatory, Big Bear City, CA 92314, USA

and

V. I. Abramenko[2]
[2]Crimean Astrophysical Observatory, 98409, Nauchny, Crimea, Ukraine

## ABSTRACT

We analyzed the $3D$ structure of the linear force-free magnetic field. A longitudinal magnetogram of the AR NOAA 8375 has been used as the photospheric boundary condition. Nov 5, 1998 2B/M8.4 two-ribbon flare can be explained in the framework of quadrupolar reconnection theory: the interaction of two closed magnetic loops which have a small spatial angle. The energy derived from SXT/YOHKOH data ($3 - 6 \times 10^{30}$ ergs) is one order of magnitude higher than the lower limit of flare energy predicted by Melrose's model. The latter estimation was made using the linear force-free extrapolation. It was suggested that taking into account a non-linear character of the observed magnetic field we can increase the lower limit of the magnetic energy stored in the studied magnetic configuration. The revealed magnetic configuration allows us to understand the observed location and evolution of the flare ribbons and the additional energy released during the gradual phase of the flare, as well. Besides, reconnection of closed magnetic loops can logically explain the connection between a two-ribbon flare and a giant X-ray post-flare arch which usually is observed after the flare onset. We emphasize that unlike the Kopp and Pneuman configuration, the model discussed here, doesn't necessarily need destabilization and opening of the magnetic field.

## 1. Introduction

It is generally accepted that a two-ribbon flare (TRF) is due to a reconnection process which happens in previously open magnetic field (Sturrock 1968, Hirayama 1974, Kopp and

Pneuman 1976). It suggests that rising prominences and/or fast expanding coronal loops are trigger of the TRF. After magnetic field destabilization and eruption, the stretched magnetic field lines become open and reconnect. This process is accompanied by type III and IV radio bursts.

On the other hand, it has also been shown that there is no direct link between filament eruption and TRF (Forbes 1992). Out of 16 studied two-ribbon flares with pre-existing dark filament, in 10 cases filaments erupted and 5 filaments remained undisturbed (Hirayama 1974). In an earlier study by Smith and Ramsey (1964), about half of the major flares were found to be associated with active region filaments and preceded by their sudden eruption.

Ogir (1967) revealed that some TRFs are not followed by type IV radio burst and their appearance in radiowaves is rather weak. Moreover, those TRFs without radio emission are different from ones which gave a radio signal. The latter type originated as one narrow chromospheric ribbon which some minutes later split up into two narrow, parallel ribbons showing a large separation, while flare ribbons in TRFs without radio emission were separated at the very beginning of the flaring process.

A simple study of H$\alpha$ images of major solar flares shows that we deal with two kinds of TRFs. The first one consists of flares with nearly parallel and straight ribbons located on opposite sides of the neutral line. Besides, footpoints of the post flare loop (PFL) system cover the entire flare ribbons (Figure 2 in Schmieder 1992, Figure 8 in Rust and Bar 1973) and the PFL system itself is in a potential state (Roy 1972) or has a more complicated structure (Rust and Bar 1973). One prominent feature of this kind of flares is the ribbon separation. Direct measurements show that the speed of the apparent expansion falls between 10 and 60 km $\cdot$ s$^{-1}$ (Ogir 1967, Hirayama 1974, Loughhead et al., 1984, Gu et al., 1992, Korobova and Sajdalieva 1993). Such TFRs might be well described by the Kopp&Pneuman configuration (Figure 1 in Kopp and Pneuman 1976).

Another kind of TRF may be described as follows. The flare ribbons are curved and not located opposite to each other. Footpoints of the post-flare loop system cover only some part of the flare ribbons (Figure 5 in Heinzel et al., 1992, Figures 2 and 3 in Tang 1985, Figure 2 and 3, present paper). The flare ribbons do not show any significant separation in the course of the flare, and at the very beginning, they are situated far from the active region neutral line (de La Beaujardiere et al. 1995). One of the flare ribbons may reach the leading sunspot and cover it partially (Figure 2 in Lin et al., 1993, Figure 1 in Gu et al., 1992).

Any flare model must explain not only how and where magnetic energy is released, but also a location, shape and a topological link between all flare ribbons and remote brightenings seen in the course of a two ribbon flare.

The Hard X-ray Imaging Spectrometer aboard the SMM mission discovered extensive post-flare coronal arches (Švestka et al., 1982). The arches appeared to be connected to the occurence of two-ribbon flares. The loops reached altitudes in excess of 150 000 km in the solar corona, and could be seen in *X-ray* for ten hours or more (Svestka 1984). These arches were either rising in the corona or stationary. Rising arches are related to CMEs while stationary ones are not (Švestka et al., 1995, Fárník et al., 1996). To explain the observed phenomena, Kopp and Poletto (1990) introduced a complex magnetic configuration which consists of two different systems of field lines that open and reconnect producing a post-flare loop system and a giant coronal arch. Simberová et al. (1993) also showed that the August 13/14, 1973 soft X-ray Skylab post-flare arch was formed by interactions of large-scale loops present above the flaring active region. This result doesn't seem to support the Kopp and Pneuman (1976) model which invokes the reconnection of the open magnetic field lines. To the contrary, the co-existence of a giant X-ray post-flare arch and a post-flare loops system in the course of a two-ribbon flare can be a sign of a single reconnection event in a simple magnetic system of closed coronal loops.

For the famous, well-studied May 16, 1981 two-ribbon flare, Vršnak et al. (1987) established that the site of energy release was located at the loop top in a closed magnetic configuration. They also conjectured that, in the studied flare, a process of driven reconnection between neighboring loops took place.

Gorbachev and Somov (1988) were first to quantitatively investigate the magnetic topology in an active region. Analyzing the potential field created by four charge points located below the photosphere, they found that the location of observed flare ribbons is in agreement with the simulations. Since then, many studies have shown that chromospheric H$\alpha$ kernels were found to be on the intersection of the separatrices (surfaces that separate volumes of different magnetic connectivity) with the photosphere. But only relatively few ones studied in detail the magnetic topology in two-ribbon flares (Gorbachev and Somov 1988, Demoulin et al., 1994a, Mandrini et al., 1995, Yurchishin 1997). Both the magnetic configuration and the H$\alpha$ brightenings are found to be qualitatively different and more complex than ones proposed in models with open magnetic field. They concluded that the flares under consideration result from the interaction of closed large-scale magnetic structures, and not from an internal instability happening within a twisted flux tube.

Recently Wang et al. (1999) analyzed the full set of ground and space based observational data and have come to the conclusion that in many aspects two-ribbon flares are different and they may represent different energy release events: eruption of sheared loops and interaction of two loops. The major morphological difference is that the former event is associated with openning of the field and the latter is not.

In this paper, we use the BBSO high resolution observation of the longitudinal magnetic field, H$\alpha$ and YOHKOH images of AR NOAA 8375, as well as a numerical method for reconstruction of the linear force-free field (LFFF) and we show that the 2B/M8.4 two-ribbon flare on Nov 5, 1998 was a result of many reconnection processes between closed magnetic loops.

## 2. Observational Data and Magnetic Field Reconstruction

BBSO observations completely covered the Nov 5, 1998 flare which occurred in AR NOAA 8375. High resolution H$\alpha$ images were obtained by the 65-cm reflector, with a 0.25 Å bandpass Zeiss filter and an OSL 12 bit camera. The cadence was 30 sec with 0.3 arcsec pixel resolution. High resolution, line-of-sight magnetograms were obtained by the 25-cm refractor. The pixel resolution was 0.5 arcsec, and the cadence 30 sec. The temporal integration of each image was 4 sec.

In our analysis, we also used the Al1 filter YOHKOH soft *X-ray* data (which covers the lower temperature range). The pixel size of SXT images was 5 arcsec.

Figure 1 shows GOES soft X-ray 1-8 Å flux plot of the Nov 5, 1998 flare as a function of time. This long duration event lasted for several hours. The flare started shortly after the very impulsive short-lasting M1.9 flare. No filament was present in this AR prior to onset, so this event is not associated with a filament eruption. Figures 2 and 3 show H$\alpha$ images obtained at the center and at the red wing of the spectral line. As one can see, it was a large flare which extended over the whole active region. The post-flare loop system connected flare ribbons $B$ and $C$ and showed apparent growth. The off-band images reveal a strong downflow at the loop footpoints. Further details on this event may be found in Wang et al. (1999).

To reconstruct coronal $3D$ magnetic field above the AR, we used a numerical method for the LFFF calculation proposed by Abramenko and Yurchishin (1996). We used the line-of-sight magnetogram of the AR 8375 as the photospheric boundary condition. The magnetogram was recorded on Nov 5, 1998 at 18:18 UT, before the flare onset. The numerical solution was obtained for a $3D$ volume of size $204 \times 204 \times 204$ arcsec. The size of a grid cell was $2.43 \times 2.43 \times 2.43$ arcsec. We obtained a set of numerical solutions with different $\alpha$ parameter and then, for each solution, we calculated the of field lines. Using high resolution BBSO H$\alpha$ images as well as soft X-ray images from YOHKOH (Figure 10 in Wang et al., 1999, Figures 2, 6 present paper), we chose the numerical solution ($\alpha = 0.013$

arcsec$^{-1}$) which best fits the observed magnetic configuration before the flare.

## 3. Results

In our analysis, we used a simple method which allowed us to define magnetic links between the flare ribbons in this two-ribbon flare.

First, we calculated, the lines of force which originate within the leading spot. The field-line calculations covered the whole sunspot area and the spatial resolution (i.e. distance between two closest footpoints of lines of force) was 2.43 arcsec in both directions. Then, considering each line, we located both its footpoints. Doing so, we could distinguish three different magnetic flux tubes. All the lines of force which originate in the area marked with $a$ have their ends at the flare ribbon marked with $B$ (line 1, Figure 4). All the field-lines starting from the area $b$ ended at the flare ribbon $A$ (lines 2, 3, Figure 4) while field-lines coming out from the area $c$ went south-eastward and ended at the H$\alpha$ brightening $D$ (Figure 5). Any two closest magnetic field lines originated correspondingly in areas $a$ and $b$, nearby to the border between them, have their second ends separated and rooted in different distant magnetic elements of northern polarity. Thus, the boundaries of these $a$, $b$, $c$ areas are the intersection of separatrices with the photosphere. In other words, following the definition by Demoulin et al. (1996), these boundaries are places where a drastic change in the field-line linkage occurs. Discontinuities in the field-line linkage at the boundary are at the origin of the formation of current sheets. It has been found that observed flare kernels are located at these discontinuities (Demoulin et al., 1996 and references therein). Our calculation show that in case of the Nov 5, 1998 flare, H$\alpha$ brightenings are also located at places where rapid changes in the field-linkage above the photosphere take place. According to this, we are able to clear up the magnetic configuration in the two-ribbon flare as well as indicate magnetic fluxes which took part in energy release process.

We suggest that there were at least three large-scale events of energy release. This comes from analysis of the GOES light curve (Figure 1), H$\alpha$ images of the AR (Figure 2) and the calculated structure of the coronal magnetic field. The first and major energy release event happened about 19:35 UT (Figure 1). The H$\alpha$ image taken at 19:43:35 UT (Figure 2) shows three well developed flare ribbons also marked on Figure 5 with letters $A$, $B$, $C$. We suppose that this energy release was due to the reconnection of two magnetic fluxes during which the connectivity of magnetic field was exchanged between four loop footpoints. The first magnetic flux is represented by a line of force *1* which connects the area $a$ and the flare ribbon $B$ and shown in Figure 4. The second one is magnetic flux which leaves the leading sunspot in the area $b$ and goes to the flare ribbon $A$ (lines of *2, 3*).

The reconnection will create new magnetic loops systems (see also schematic representation of the magnetic configuration in Figure 8). The first one, the H$\alpha$ post-flare loop system connects the area $b$ and the flare ribbon $B$ (Figure 4), while the second one, a large scale loop system, connects the area $a$ and the flare ribbon $A$. This large-scale loop might corresponds to a well-known giant X-ray post-flare arch (Švestka et al., 1982). Figure 6 shows the off-band H$\alpha$ image (the same as in Figure 3) with an overlapped SXT/YOHKOH image. One clearly sees the presence of both the low-lying H$\alpha$ post-flare loop system (dark loops) and the overlaying hot *X-ray* giant coronal arch (a white loop with contours at the right top corner). The H$\alpha$ loop are located just below the hot *X-ray* loop with their top being almost tangential. The post flare loop system connects the leading sunspot and the flare ribbon $B$ and the large scale *X-ray* arch has its footpoints at the sunspot and the flare ribbon $A$. This kind of magnetic connection corresponds to that predicted by the model. Figure 7 shows the same YOHKOH image with the giant post-flare arch with overplotted calculated lines of force. The parameter $\alpha$ was equal, in this calculation, to 0.001 arcsec$^{-1}$. Thus, the observed magnetic configuration entirely supports the inferences obtained from the modeled representation of the magnetic field in the AR.

Both, the post flare loops system and the giant X-ray post-flare arch exhibit apparent growth ( Poletto and Švestka 1992, Schmieder et al., 1995, van Driel-Gesztelyi et al., 1997) as the flare is in progress. Thus, due to the evolution of newly formed loops, a disturbance of the pre-existing overlaying magnetic field will take place. This, in turn, might provoke the subsequent reconnection of the newly formed loops with the loops system which connects the area $c$ and the flare ribbon $D$ (Figure 5). If we are correct, this second-step reconnection should start a bit later than the main phase of the energy release. This might be seen in H$\alpha$ images taken at 19:43 UT and 20:29 UT (Figure 2). One may see that when the eastern ribbon (marked with $A$ in Figures 2) has faded, the south-east ribbon (marked with $D$) became brighter. Also, according to SGD (Figure 1), at 20:30 UT, after the X-ray flux reached its maximum, the GOES light curve has broken its gradual decrease and has formed plateau which might imply that an additional source of energy has turned on. This second reconnection event creates a new loop system connecting the area $c$ with the flare ribbon $A$ and $b$ with $D$ (Figure 5) and explains the evolutin aof the flare ribbons.

As it follows from Figure 8$c$ that there is also a possible third reconnection process which involves magnetic loops $aA$ and $bD$. After all these steps, the reconnection will be completed and the magnetic field configuration will consist of new disjoint loops (Figure 8$d$) and the magnetic field will have a lower amount of energy than to the pre-flare state. The observed evolution of the flare ribbons seems to support the proposed scenario.

A specific feature of this type of reconnection is the exchange of the connectivities of opposite magnetic polarities without a significant change in the longitudinal field. Analysis of the longitudinal magnetograms supports this theoretical assumption since no large-scale magnetic flux cancellations at, or around, the flare site were observed (Wang et al., 1999).

## 4. Discussion and Conclusion

The reconnection model of Heyvaerts et al. (1977) suggests a reconnection of oppositely-directed fields. Nevertheless, it had been pointed out (Hanaoka 1996) that the observed, interacting flare loops were not necessarily oriented in an anti-parallel direction. Moreover, the null points are presented in the magnetic field above the photosphere only when the parasitic bipole is nearly parallel to the large-scale overlaying magnetic field (Demoulin et al., 1994b) which can produce a simple loop flare (Heyvaerts et al., 1977). However, configurations without the nulls above the photosphere level could also produce flares (Demoulin et al., 1994b). In the absence of the null point in the magnetic field configuration, Berger (1988), Priest (1988) and then Priest and Forbes (1992) have proposed that the $3D$ magnetic reconnection may occur at the separatrix layers (Demoulin et al., 1996; Longcope 1996). The typical configuration consists of a pair of two unequally sized loops. The closer footpoints share the same magnetic polarity while the loop planes make some angle in space (Hanaoka 1996, 1997, Nishio et al., 1997, Anschwanden et al., 1999). The magnetic configuration in this interaction can be described in terms of the quadrupolar configuration (Anschwanden et al., 1999). The only possible way for relaxting the pre-existing magnetic field is to exchange the connectivities of opposite magnetic polarities. The resulting configuration will consist of two disjoint magnetic loops, and will be simplified with reduced differential shear (Schmieder et al., 1996, Abramenko and Yurchishin 1998). This process is in agreement with our present understanding of the evolution of an active region as a continual distortion of an existing equilibrium of the magnetic field with a subsequent fast relaxation to a new neighboring equilibrium (Hayvaerts and Priest 1984, Longcope 1996).

Recently Anschwanden et al. (1999) studied in great detail quadrupolar magnetic reconnection in solar flares. One finding is that out of 10 studied solar flares 6 are found with almost collinear interacting loops (the angle between these loops was less then $16°$). Another interesting result is based on Melrose's (1997) flare model. It has been estimated that only a self-inductance of the largest magnetic loop involved in reconnection is relevant for the free magnetic energy. Amount of the energy depends, to first order, on the length of the largest loop and the current ratio $I_1/I_2$ of two interacting loops. The angle between interacting magnetic field lines and their relative distance was found to be of much less importance. The flare energy estimated on the basis of Melrose's model closely matches the energy inferred from GOES SXR flux and HXT hard X-ray flux (Anschwanden et al., 1999).

The radiative energy from the SXR emitting plasma for the Nov 5, 1998 flare, can be estimated by:

$$\Delta E^{SXT} = 3kTn_e fV$$

or,

$$\Delta E^{SXT} = 3kT\sqrt{fVEM},$$

where $T$ is the plasma temperature, $n_e$ and $v$ are the electron density and the emitting volume correspondingly, and $f$ is the filling factor of the SXR loops, $f \leq 1$. $k$ is the Boltzmann constant. EM is the Emission Measure of the plasma which can be expressed as: $EM = \int n^2 V$. The plasma parameters can be determined from GOES two-channel diagnostics and the loop morphology observed by SXT and TRACE.

The maximum temperature of the hot plasma was recorded as 20MK, and the Emission Measure (EM) of the SXR plasma was $1\times10^{50}$ cm$^{-3}$. The length and width of the SXR loops can be estimated from SXT and TRACE images, and the thickness of the loop(s) is taken the same as the loop width, hence the emitting volume V is estimated to be $9\times10^{27}$ cm$^3$. Taking the filling factor as 1, the electron density of the loops was about $1\times10^{11}$ cm$^{-3}$. The radiative energy contained in the SXR plasma is thus obtained as 4-7$\times$ $10^{30}$ erg, if the filling factor is chosen to vary between 0.3-1.

To estimate the lower limit of the energy released in the Nov 5, 1998 flare we made use of our extrapolated field and Anschwanden et al. (1999)'s adoption of the Melrose's quadrupolar current-loop model. It suggests that the energy released in the flares is due to a redistribution of electric currents and the magnetic flux above the photosphere. The maximum transferable flare energy is defined as

$$\Delta E \approx L_2 (\frac{I_2}{I_1})^2 \approx 10^{29.63} (\frac{r_2}{10^9 cm})(\frac{I_2}{10^{11} A})^2 \text{ erg},$$

where $r_2$ and $I_2$ are the radius and the current of the large-scale field line involved in the reconnection Anschwanden et al. (1999). From Figure 4, we estimated the radius $r_2$ as half the distance between the flare ribbon $A$ and the area $b$, and it is equal to $40'' = 3 \times 10^9$ cm. Unfortunately, we do not have transverse magnetograms for this AR. To estimate the lower limit of the current $I_2$, flowing in the large-scale loop, connecting the area $b$ and the flare ribbon $A$, we used a linear force-free field transverse magnetogram. Thus, we have obtained the value of the current $I_2$ equal to $5 \times 10^{10} A$. This parameters gave us the value of $\Delta E = 7.5 \times 10^{29}$ erg which is one order lower then the observational estimates based on the YOHKOH/SXT irradiation. The estimation was made assuming the linear force-free magnetic field with $\alpha = \text{const}$. In this case, the net current $I$ is equal to the total current $I_2$ of some sign (depends on sign of $\alpha$) flowing in coronal loop. However, taking into account the non-linear character of observed solar magnetic fields and the small-scale structure of the coronal electric currents, it is strightforward to assume that stronger currents are present in coronal loops. Indeed, let's consider a coronal loop which has a non-linear internal structure with an oscillating $\alpha$ parameter (parameter of the non-linear force-free field $\alpha$ takes positive and negative values inside the loop). The net current $I = I_2^+ + I_2^-$ flowing in a coronal loop defines its large-scale structure, in particular, the location of both its footpoints. Then, we can increase or decrease, to some extend, a total positive and a negative currents $I_2^+$ and $I_2^-$, keeping the net current $I$ constant. It would give us unchanged shape of the coronal loop and the constant location of its footpoints, while the internal structure would be more twisted or relaxed. That is the one possible way to increase an amount of currents in a coronal loop. For instance, if we increase the $I_2^+$ or $I_2^-$ current only by factor of 2, the flare energy $\Delta E$ would be equal to $3 \times 10^{30}$ erg, which is exactly what we have obtained from the YOHKOH observations.

As inferred from LFFF modeling, the two-ribbon flare on Nov 5, 1998 was a product of multiple reconnection process between interacting loops which make a small angle in space. Calculations presented here explore only the large-scale magnetic field structure in the AR. However, taking into account a possible filamentation of the solar magnetic field, this flare could be considered as a superposition of many small-scale reconnection events. In this case, one would expect a variety of angles between small-scale magnetic fluxes which would bring up the additional energy for the flare (Anschwanden et al., 1999). Another possible scenario is that the self-organized criticality model could be realized with the avalanche process of small-scale energy releases (Lu and Hamilton 1991; Georgoulis and Vlahos 1996).

The magnetic configuration, revealed here, naturally explains the location and the shape of the flare ribbons, the location of the post flare loop system, as well as the magnetic connection between the H$\alpha$ brightenings. Multiple magnetic reconnection also allows us to explain the evolution of the flare ribbons and the additional energy release during the gradual phase of the flare.

The interaction of closed magnetic loops in two-ribbon flare can also explain the origin of the giant X-ray coronal arch observed after the two ribbon flare onset (Švestka et al., 1982). This result also meets the Šimberova et al. (1993)'s conclusion that the giant arch is the result of progressive reconnection of elementary flux tubes of two (or more) interacting loops.

We would like to emphasize that unlike the Kopp&Pneuman configuration, the model discussed here does not necessarily need destabilization and eruption of the active region filament. The filament eruption, even if it accompanies a two-ribbon flare, could be a one of many equal possibilities to trigger a solar flare.

We acknowledge the referee's comments and suggestions that helped our improving the peresentation. This work was supported in part by NSF-ATM (97-14796) and NASA (NAG5-4919) grants.

## 5. References

Abramenko, V.I., and Yurchishin, V.B. 1996, Sol. Phys., 168, 47.

Abramenko, V.I., and Yurchishin, V.B. 1998, in 2nd Advances in Solar Physics Euroconference, Three-Dimensional Structure of Solar Active Rgions, ed. C. Alissandrakis, and B. Schmieder, AS. Conf. Ser. 155, 85.

Aschwanden, M.J., Kosugi, T., Hanaoka, Y., Nishino, M., and Melrose, D.B. 1999, ApJ, accepted.

Berger, M.A. 1988, Proceedings of an International Workshop on Reconnection in Space Plasmas, ESA SP-285, Vol. II, 83.

de la Beaujardiere, J.-F., Canfield, R.C., Hudson, H.S., Wulser, J.-P., Acton, L.W., Kosugi, T., and Masuda, S. 1995, ApJ, 440, 386

Demoulin, P., Mandrini, C.H., Rovira, M.G., Henoux, J.-C., and Machado, M.E. 1994a, Sol. Phys., 150, 221.

Demoulin, P., Henoux, J.C., and Mandrini, C.H.: 1994b, A&A, 285, 1023.

Demoulin, P., Henoux, J.C., Priest, E.R., and Mandrini, C.H. 1996, A&A, 308, 643.

Fárník, F., Švestka, Z., Hudson, H.S., and Uchida, Y. 1996, Sol. Phys., 168, 331.

Forbes, T.G., 1992, in Lecture Notes in Physics: Eruptive Solar Flares, ed. Z. Švestka, B.V. Jackson, and M.E. Machado, 79

Georgoulis, M.K., and Vlahos, L. 1996, ApJ, 469, L135.

Gorbachev, V.S., and Somov, B.V. 1988, Sol. Phys., 117, 77.

Gu, X.-M., Lin, J., Luan, T., and Schmieder, B. 1992, A&A, 259, 649.

Hanaoka, Y. 1996, Sol. Phys., 165, 275.

Hanaoka, Y. 1997, Sol. Phys., 173, 319.

Heinzel, P., Schmieder, B., and Mein, P. 1992, Sol. Phys., 139, 81.

Heyvaerts, J., and Priest, E.R. 1984, A&A, 137, 63.

Heyvaerts, J., Priest, E.R., and Rust D. 1997, ApJ, 216, 123.

Hirayama, T. 1974, Sol. Phys., 34, 323.

Hishio, M., Yaji, K., Kosugi, T., Nakajima, H., and Sakurai, T. 1997, ApJ 489, 976.

Kopp, R.A., and Pneuman, G.W. 1976, Sol. Phys., 50, 85.

Kopp, R.A., and Poletto, G. 1990, Sol. Phys., 127, 267.

Korobova, Z.B., and Sajdalieva, M.A. 1993, Sol. Phys., 147, 323.

Lin, Y.-Z., Zhang, H.-Q., and Zhang W.-J. 1993, Sol. Phys., 146, 135.

Longcope, D. W., 1996, Sol. Phys., 169, 91

Loughhead, R.E., Chen C.-L., and Wang, J.-L. 1984, Sol. Phys., 92, 53.

Lu, E.T., and Hamilton R.J.:1991, ApJ, 380, L89.

Mandrini, C.H., Demoulin, P., Rovira, M.G., de La Beaujardière, and Henoux J.-C. 1995, A&A, 303, 927.

Melrose, D.B. 1997, ApJ, 486, 521.

Ogir, M.B. 1967, Bull. Crimean Astrophys. Obs., 37, 94.

Poletto, G., and Švestka, Z.F. 1992, Sol. Phys., 138, 189.

Priest, E.R. 1988, Proceedings of an International Workshop on Reconnection in Space Plasmas, ESA SP-285, Vol. II, 73.

Priest, E.R., and Forbes, T.G. 1992, J. Geophys. Res., 97(A2), 1521.

Roy, J.-R. 1972, Sol. Phys., 26, 418.

Rust, D. M., and Bar, V. 1973, Sol. Phys., 33, 459.

Sams, III, B. J., Golub, L., and Weiss, N.O. 1992, ApJ, 399, 313.

Schmieder, B., 1992, in Lecture Notes in Physics: Eruptive Solar Flares, ed. Z. Švestka, B.V. Jackson, and M.E. Machado, 124.

Schmieder, B., Heinzel, P., Wiik, J. E., Lemen, J., Anwar, B., Kotrc, P., and Hiei, E. 1995, Sol. Phys., 156, 337.

Schmieder, B., Demoulin, P., Aulanier, G., Golub, L. 1996, ApJ, 467, 881.

Šimberova, S., Karlicky, M., and Švestka, Z. 1993, Sol. Phys., 146, 343.

Smith, S.F. and Ramsey, H.E. 1964, Z. Astrophys. 60, 1.

Sturrock, P.A., 1968, in IAU Symp. 35: Structure and Development of Solar Active Regions, ed. K.O. Kiepenheuer, 471.

Švestka, Z., Stewart, R.T, Hoyng, P., van Tend, W., Acton, L.W., Gabriel, A.H., Rapley, C.G., and 8 coauthors: 1982, Sol. Phys., 75, 305.

Švestka Z. 1984, Sol. Phys., 94, 171.

Švestka, Z., Fárník, F., Hudson, H.S., Uchida, Y., Hick, P., and Lemen, J. 1995, Sol. Phys., 161, 331.

Tang, F. 1985, Sol. Phys., 102, 131.

Vršnak, B., Ruždjak, V., Messerotti, M., and Zlobec, P. 1987, Sol. Phys., 111, 23.

Wang, H., Goode, Ph.R., Denker, C., Yang, G., Yurchyshyn, V., Nitta, N., Gurman, J. B., Cyr, C. St., Kosovichev, A.G. 1999, ApJ, submitted

Yurchishin, V.B. 1997, Kinematics Phys. Celest. Bod., 13, N6, 33.

## Figure Caption

Fig. 1.— GOES X-ray time profile of November 5, 1998 flare.

Fig. 2.— H$\alpha$ images of the two-ribbon flare obtained on November 5, 1998. The imeges are from 65-cm telescope, the field of view is 200 by 200 arcsec.

Fig. 3.— H$\alpha$ off-band images of the two-ribbon flare on November 5, 1998. The image at 20:56:35 UT is a contrast enhanced image. The flare ribbons appear brighter then it was observed.

Fig. 4.— Location of H$\alpha$ flare ribbons (dashed area) superposed on a contour map of the longitudinal magnetic field (solid lines - N polarity, dashed - S polarity). Contours levels are 100, 200, 400, 800 G. Solid lines 1, 2, 3 denote calculated field-lines ($\alpha = 0.013 arcsec^{-1}$) connecting the areas $a$ and $b$ with the flare ribbons $A$ and $B$.

Fig. 5.— H$\alpha + 0.75$Å image taken at 20:56:35 UT. Dark loops at upper right – growing post-flare loops system (PFL). Solid lines denote calculated field-lines connecting the area $b$ with the flare ribbon $A$. Dashed lines – calculated field lines ($\alpha$ = 0.013 arcsec$^{-1}$) which connect the area $c$ with the flare ribbon $D$.

Fig. 6.— H$\alpha$+0.75Å image overlapped by a soft X-ray YOHKOH image shows the magnetic configuration after the flare. The resultion configuration consists of the low-laying post-flare loops system (dark loops) and the overlaying giant X-ray post-flare arch. The crosses denote the hottest parts of H$\alpha$ and X-ray loops and might locate the site of the reconnection.

Fig. 7.— Soft X-ray YOHKOH image and the lines of force of the linear force-free field. Parameter $\alpha = 0.001$ arcsec$^{-1}$

Fig. 8.— A sketch of possible sequence of events occurred in November 5, 1998 two-ribbon flare. The "$\times$" marks the site of reconnectin. The letters denote the loop footpoints and the flare ribbons according to observed picture (see Figures 3 and 4).

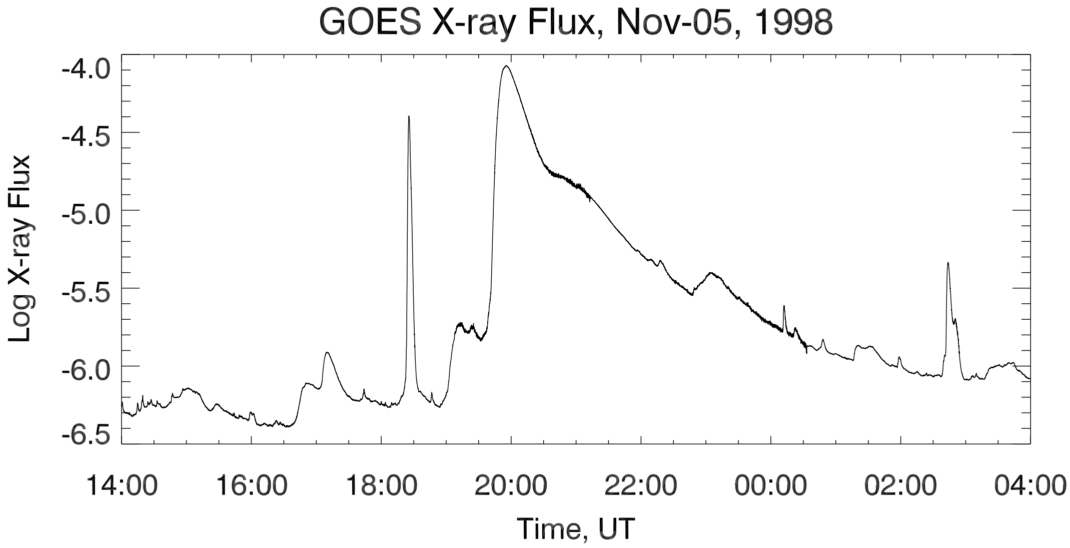
GOES X-ray Flux, Nov-05, 1998
Log X-ray Flux
-4.0
-4.5
-5.0
-5.5
-6.0
-6.5
14:00
16:00
18:00
20:00
22:00
00:00
02:00
04:00
Time, UT

Fig. 1.

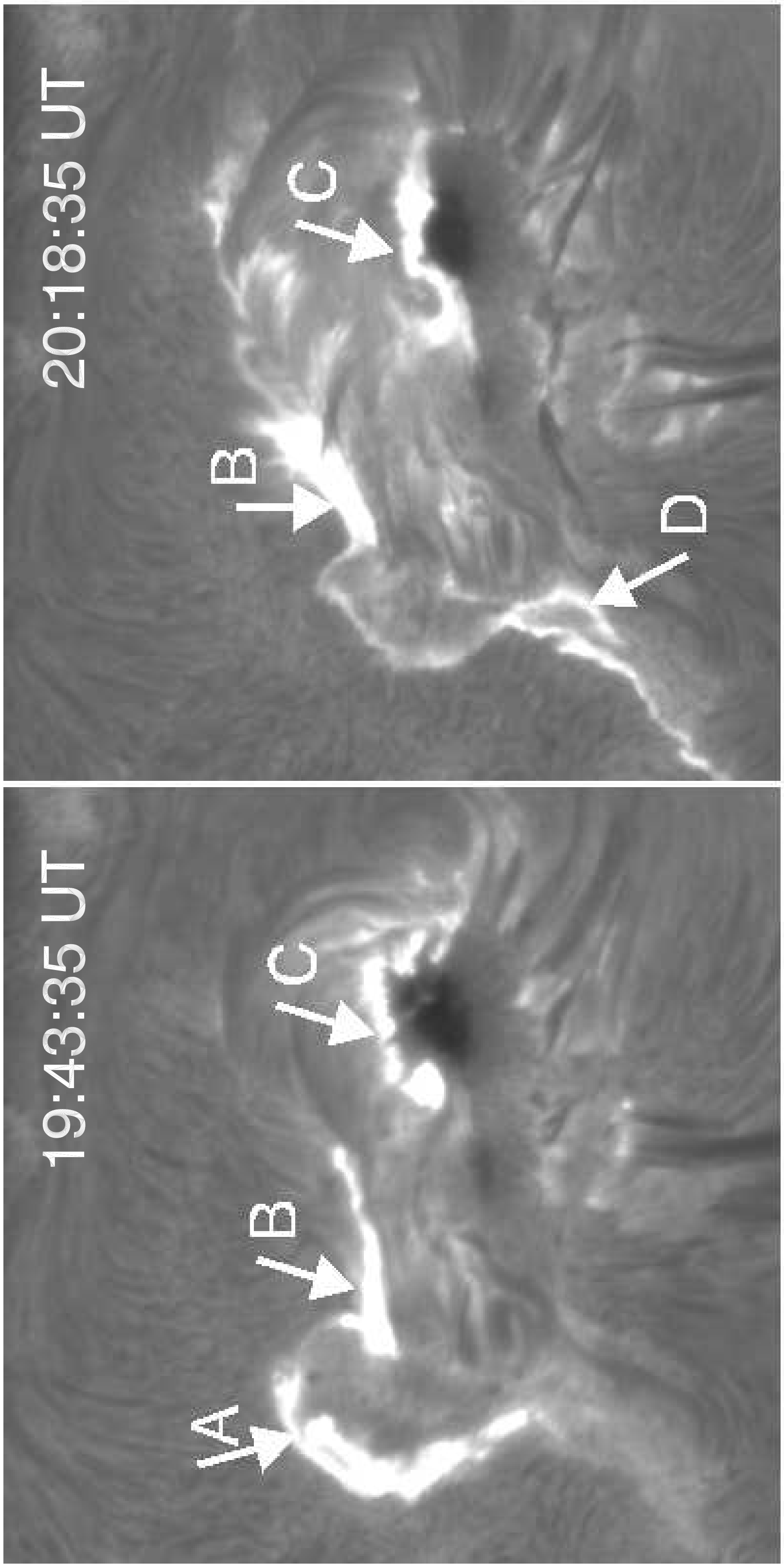


Fig. 2.

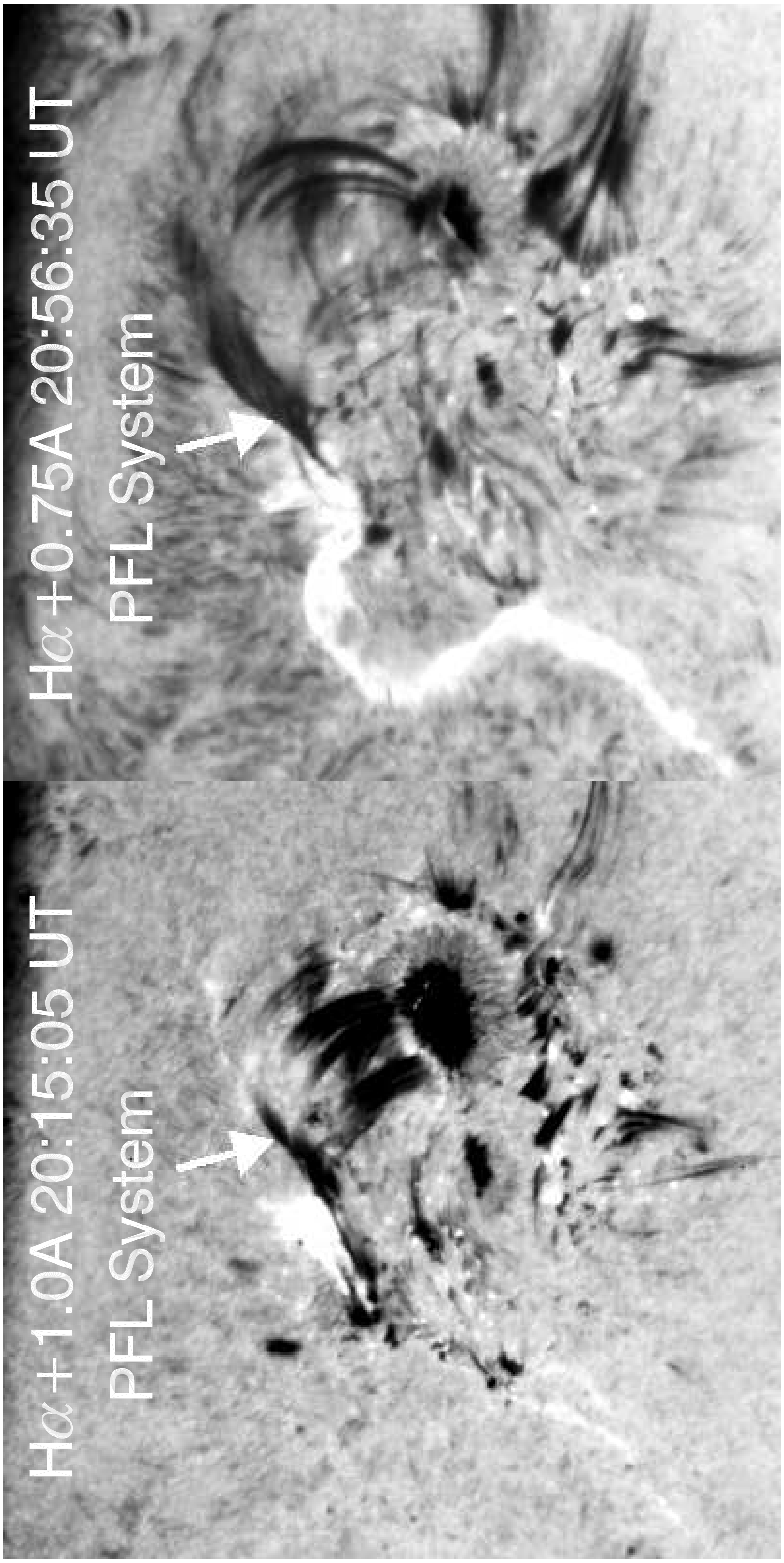


Fig. 3.

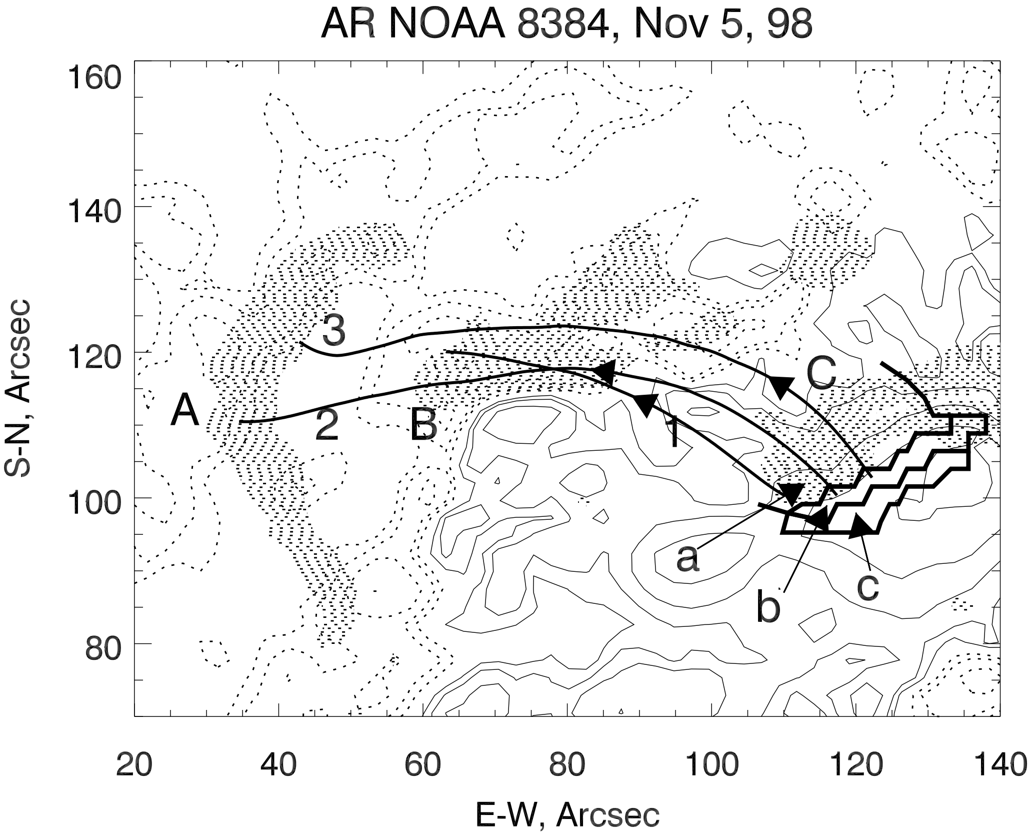
AR NOAA 8384, Nov 5, 98
S-N, Arcsec
E-W, Arcsec
160
140
120
100
80
20
40
60
80
100
120
140
A
B
C
1
2
3
a
b
c

Fig. 4.

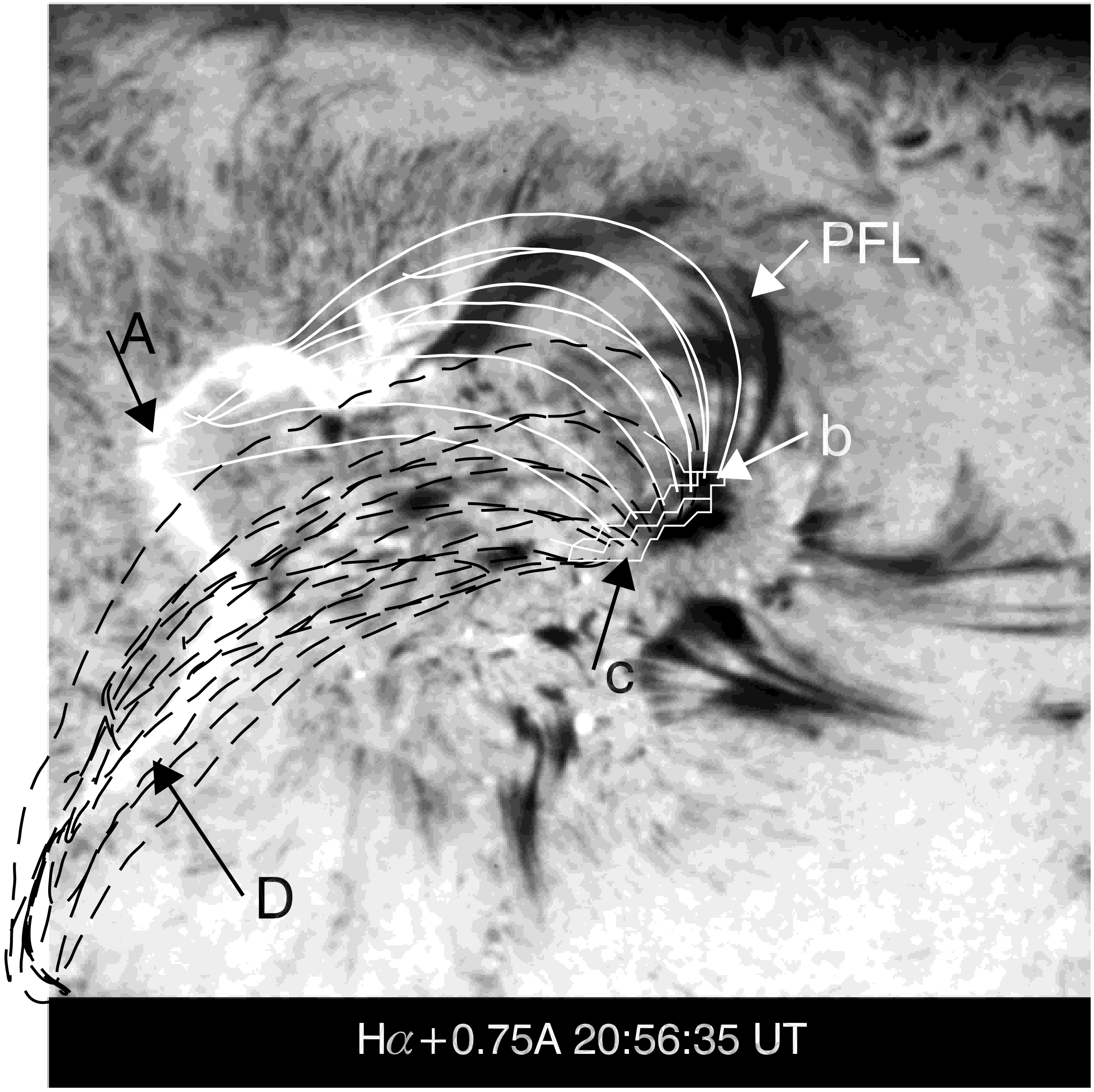


Fig. 5.

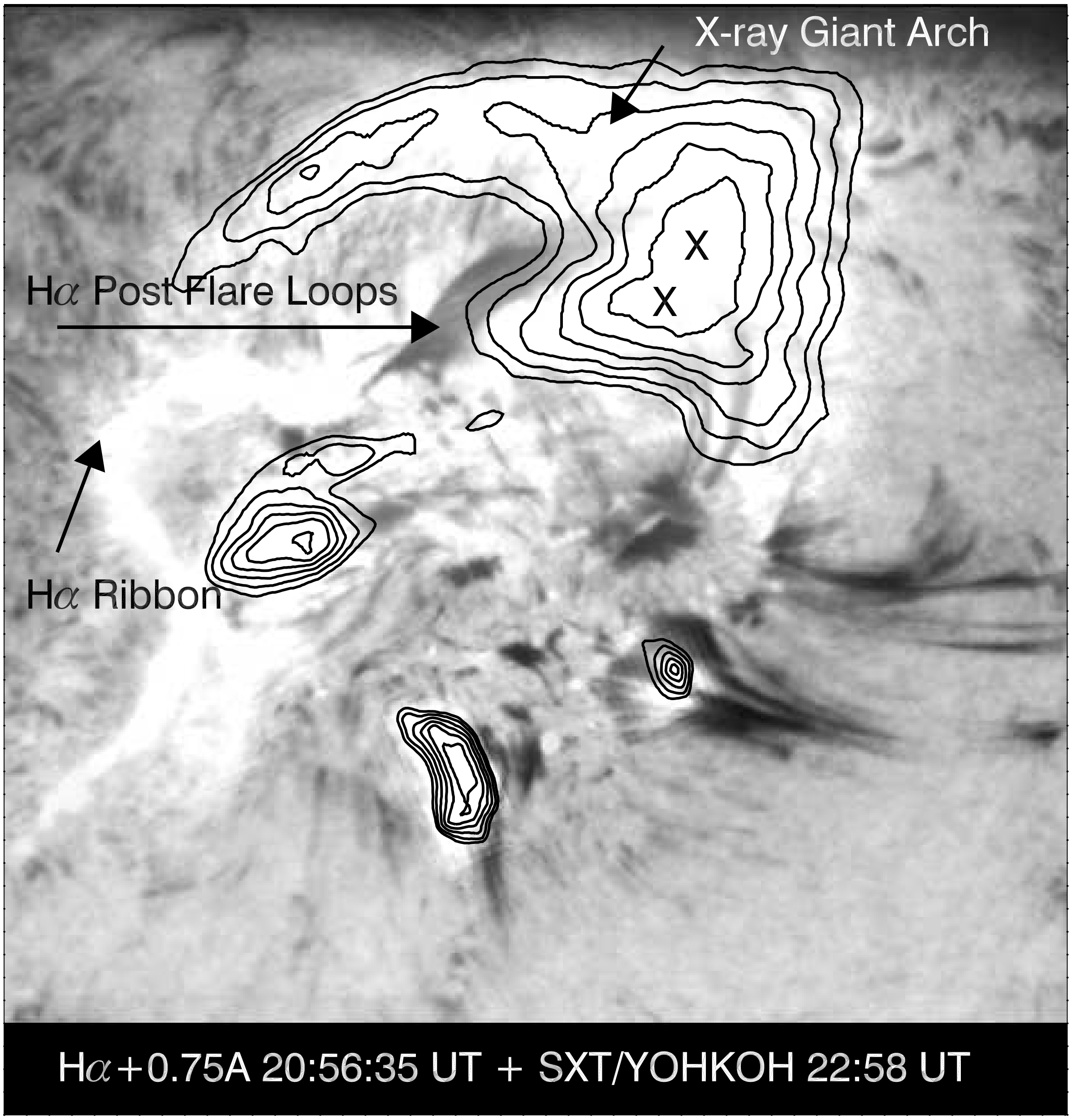
X-ray Giant Arch
X
X
Hα Post Flare Loops
Hα Ribbon
Hα+0.75A 20:56:35 UT + SXT/YOHKOH 22:58 UT

Fig. 6.

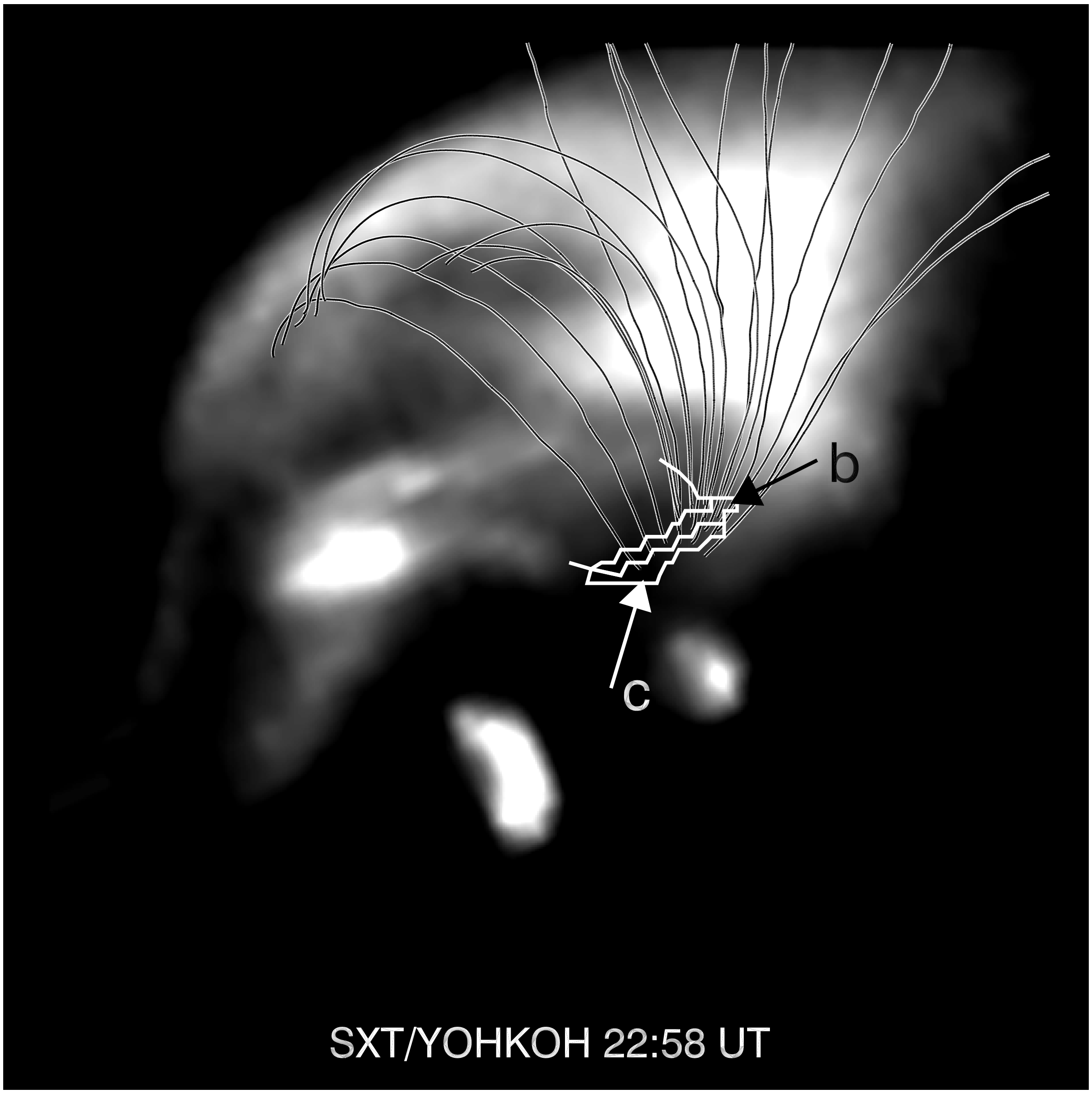


Fig. 7.

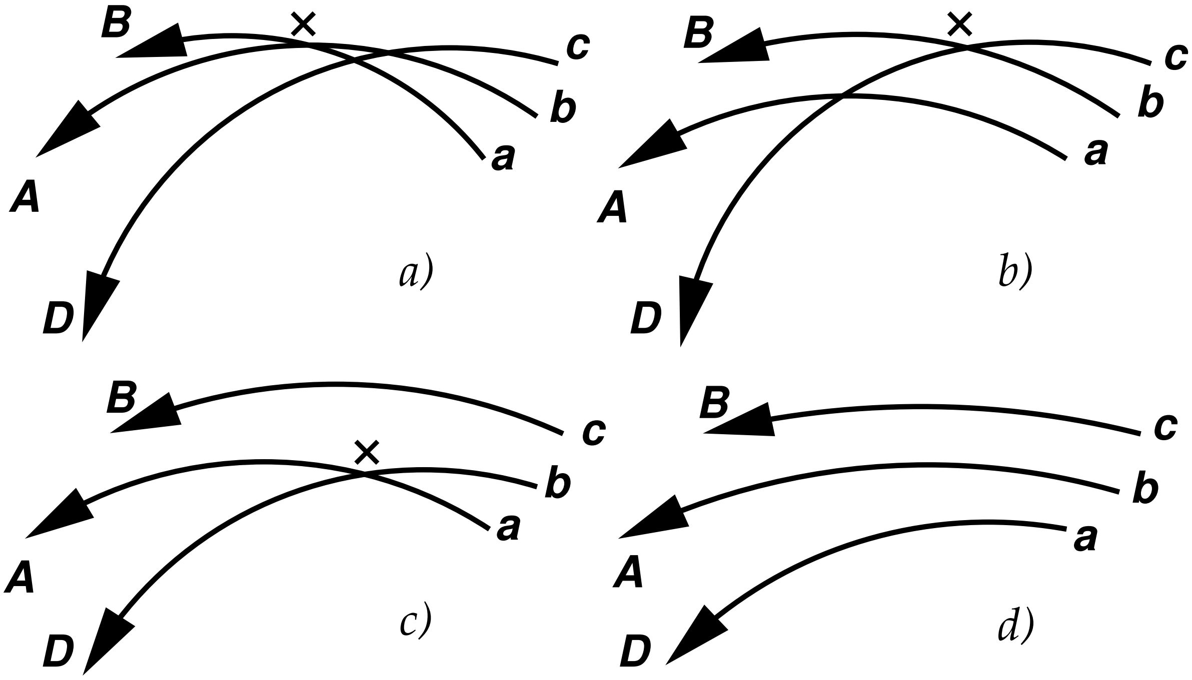


Fig. 8.